Numerical solution of the two-dimensional Helmholtz equation with variable coefficients by the radial integration boundary integral and integro-differential equation methods

M. A. AL-Jawary and L. C. Wrobel
School of Engineering and Design, Brunel University, Uxbridge UB8 3PH, UK
E-mails: Majeed.AL-Jawary@brunel.ac.uk; Luiz.Wrobel@brunel.ac.uk;

Abstract. This paper presents new formulations of the boundary-domain integral equation (BDIE) and the boundary-domain integro-differential equation (BDIDE) methods for the numerical solution of the two-dimensional Helmholtz equation with variable coefficients. When the material parameters are variable (with constant or variable wave number), a parametrix is adopted to reduce the Helmholtz equation to a BDIE or BDIDE. However, when material parameters are constant (with variable wave number), the standard fundamental solution for the Laplace equation is used in the formulation. The radial integration method is then employed to convert the domain integrals arising in both BDIE and BDIDE methods into equivalent boundary integrals. The resulting formulations lead to pure boundary integral and integro-differential equations with no domain integrals. Numerical examples are presented for several simple problems, for which exact solutions are available, to demonstrate the efficiency of the proposed methods.

Keywords: Helmholtz equation, boundary integral equation method, boundary integro-differential equation method, variable coefficients, parametrix, radial integration method

1 Introduction

The Helmholtz equation is widely used to model many problems in physics and mechanics. If the material is homogeneous and there are no source/sink terms, then the governing equation is the homogeneous Helmholtz equation [1, 2]. When source terms are present, however, a non-homogeneous Helmholtz equation must be considered. Numerical solutions of these problems have been obtained by means of the finite element method (FEM) and the finite difference method (FDM).

The boundary element method (BEM) is based on the reformulation of the partial differential equation into an integral equation on the domain boundary only [3–6]. The main features which render the BEM advantageous with respect to FEM and FDM are the reduction of the problem dimensions by one and the fact that no discretization of the computational domain is required.

Rangogni [2] presented a BEM formulation for the non-homogeneous Helmholtz equation with harmonic source terms, and the domain integral transformed to a boundary integral using Green's formula. The BEM for a non-homogeneous Helmholtz equation with variable coefficients is discussed in [1]. The authors used the fundamental solution for the Laplace equation to transform the non-homogeneous Helmholtz equation to a boundary integral equation, and then an iteration method was used to solve the BIE. A comparative study of BEM and FEM for the Helmholtz equation in two dimensions is performed in [7]; the numerical investigations showed that the BEM is generally more accurate than the FEM when the size of the finite elements is comparable to that of the boundary elements, especially for the Dirichlet problem.

BEM formulations for solving non-linear, non-homogeneous problems and problems with variable coefficients usually adopt fundamental solutions for a simplified linear, homogeneous problem with constant coefficients, generating domain integrals in the corresponding integral equation. This feature makes the BEM less attractive as a domain discretisation is then required.

Several methodologies have been proposed in order to overcome these difficulties. One possible technique is to find a fundamental solution for the non-linear, non-homogeneous problem or problem with variable coefficients which can provide a pure boundary integral equation. Unfortunately, these fundamental solutions are only available for some very special cases [8–11].

An alternative methodology for solving PDEs with variable coefficients with the BEM without domain discretisation involves the transformation of the domain integrals appearing in the integral equation, derived by using fundamental solutions for linear homogeneous problems, into equivalent boundary integrals. There are two powerful techniques available in literature: the first is the dual reciprocity method (DRM) developed by Nardini and Brebbia [12]. In this method, the transformation is carried out by approximating the body force term with a series of basis functions and by using their particular solutions. A detailed description and practical applications of this method can be found in the book of Partridge et al. [13]. The drawback of this technique is that the particular solutions may be difficult to obtain for some complicated problems, depending on the radial basis function (RBF) adopted. In addition, even for known body forces, the method still requires an approximation of the known function using RBFs [14].

More recently, a new transformation technique, the radial integration method (RIM), has been developed by Gao [14, 15] . The RIM can transform any complicated domain integral to the boundary, while also removing various singularities appearing in the domain integrals. The main feature of the RIM is that it can treat different types of domain integrals in a unified way since it does not resort to particular solutions as in the DRM.

Another methodology for solving PDEs with variable coefficients is to use a parametrix (Levi function), which is usually available [16,17]. This allows a reduction of the mathematical problem to a boundary-domain integral or integro-differential equation (BDIE or BDIDE) [18–22]. AL-Jawary and Wrobel [18–20] have successfully implemented BDIE and BDIDE formulations for stationary heat transfer in isotropic materials with variable coefficients associated with Dirichlet, Neumann and mixed boundary conditions. The numerical results show that high rates of convergence are obtained with mesh refinement.

A BDIE and a BDIDE formulations for stationary heat transfer with variable coefficients are presented in [21] using specially constructed localised parametrices to reduce the BVP to a localised boundary-domain integral or integro-differential equation (LBDIE or LBDIDE). The use of specially constructed localised parametrices leads to sparsely populated systems of linear algebraic equations. An implementation of the LBDIE method for the numerical solution of a second-order linear elliptic PDE with variable coefficients is presented in [22], although the formulation is restricted to Neumann boundary-value problems.

In the present paper, the BDIE and BDIDE formulations proposed by Mikhailov for the Laplace equation [21] are extended to the treatment of the two-dimensional Helmholtz equation when the material parameters and wave number vary within the medium. Moreover, a new type of boundary-only integral equation technique is developed. Herein, the RIM is used to convert the domain integrals appearing in both BDIE and BDIDE to equivalent boundary integrals. For domain integrals consisting of known functions the transformation is straightforward, while for domain integrals that include unknown variables the transformation is accomplished with the use of augmented RBFs, similar to the DRM. The most attractive feature of the method is that the transformations are very simple and have similar forms for both 2D and 3D problems. Modifications have been introduced to the RIM developed by Gao [23] in its application to the BDIE and BDIDE formulations, particularly the fact that the radial integral is calculated by using a transformation proposed by Fata [24] which produces a pure boundary-only formulation and relaxes the "star-shaped" requirement of the RIM as the straight path from the source point to any field point will always exist. Some numerical examples are given to demonstrate the efficiency of the proposed methods.

2 Reduction of the Helmholtz equation with variable coefficients to a BDIE/BDIDE

Let us consider the following non-homogeneous Helmholtz equation with variable coefficients for a two-dimensional body Ω. In the direct problem formulation, the acoustic pressure $\bar{u}(x)$ is prescribed on part $\partial_D\Omega$ of the boundary $\partial\Omega$ and the normal velocity $\bar{t}(x)$ on the remaining $\partial_N\Omega$ part of $\partial\Omega$, see [2, 3, 25]

$$(Lu)(x) := \sum_{i=1}^{2} \frac{\partial}{\partial x_i}\left[a(x)\frac{\partial u(x)}{\partial x_i}\right] + k(x)u(x) = f(x) \qquad x \in \Omega \tag{1}$$

with the mixed boundary conditions

$$u(x) = \bar{u}(x), \qquad x \in \partial_D\Omega \tag{2}$$

$$Tu(x) = \bar{t}(x), \qquad x \in \partial_N\Omega \tag{3}$$

where Ω is a bounded domain, $a(x)$ is a known variable material coefficient, $f(x)$ is a given function; $x = (x_1, x_2)$; $k(x)$ is a known variable wave number, $[Tu](x) := a(x)\frac{\partial u}{\partial n}(x)$, $n(x)$ is the external normal vector to the boundary $\partial\Omega$, and $\bar{u}(x)$ and $\bar{t}(x)$ are known functions. We assume that $k(x)$ is not an eigenvalue for the homogeneous form of the mixed problem (1)-(3).

The Green formula for the differential operator L has the form

$$\int_\Omega [uL\varphi - \varphi Lu]d\Omega = \int_{\partial\Omega} [uT\varphi - \varphi Tu]d\Gamma \tag{4}$$

where u and φ are arbitrary functions.

Assume L to be a linear operator with constant coefficients and $F(x, y)$ its fundamental solution, i.e.

$$L_x F(x, y) = \delta(x - y)$$

where $y = (y_1, y_2)$ is a source point, and δ is the Dirac delta function. Then one could take $\varphi(x) = F(x, y)$, identify $u(x)$ with a solution of Eq.(1) with constant $a(x)$ and $k(x)$, and thus arrive at the third Green identity

$$c(y)u(y) - \int_{\partial\Omega} [u(x)T_x F(x, y) - F(x, y)Tu(x)]d\Gamma = \int_\Omega F(x, y)f(x)d\Omega(x) \tag{5}$$

where

$$c(y) = \begin{cases} 1 & \text{if } y \in \Omega \\ 0 & \text{if } y \notin \bar{\Omega} \\ \frac{\alpha(y)}{2\pi} & \text{if } y \in \partial\Omega \text{ and } \Omega \subset \mathbb{R}^2, \end{cases} \tag{6}$$

where F is the fundamental solution to the Helmholtz equation and $\alpha(y)$ is the interior angle at a point y of the boundary $\partial\Omega$, particularly, $c(y) = 1/2$ if y is a smooth point of the boundary [3–5].

For partial differential operators with variable coefficients, like L in Eq.(1), a fundamental solution is generally not available in explicit form. However, a parametrix is often available instead, which is a function $P(x, y)$ satisfying the equation [18–22],

$$L_x P(x, y) = \delta(x - y) + V(x, y), \tag{7}$$

where $V(x, y)$ is the remainder which has no more than a weak (integrable) singularity at $x = y$. The fundamental solution of the operator with "frozen coefficients" corresponding to the operator L defined in (1) can be used as a parametrix, in the $2D$ case [18–22],

$$P(x,y) = \frac{1}{2\pi a(y)} \ln|x-y| \tag{8}$$

Substituting Eq.(8) in Eq.(7), the remainder $V(x,y)$ will then be [18–22],

$$V(x,y) = \sum_{i=1}^{2} \frac{x_i - y_i}{2\pi a(y)|x-y|^2} \frac{\partial a(x)}{\partial x_i}, \quad x,y \in \mathbb{R}^2 \tag{9}$$

Substituting $P(x,y)$ for $\varphi(x)$ in Eq.(4) and taking $u(x)$ as a solution to Eq.(1), we obtain the integral equality,

$$c(y)u(y) - \int_{\partial\Omega} [u(x)T_x P(x,y) - P(x,y)Tu(x)]d\Gamma(x) + \int_{\Omega} V(x,y)u(x)d\Omega(x) + \\ + \int_{\Omega} k(x)P(x,y)u(x)d\Omega(x) = \int_{\Omega} P(x,y)f(x)d\Omega(x), \tag{10}$$

Now, we can multiply both sides of Eq.(10) by $a(y)$ to obtain:

$$a(y)c(y)u(y) - \int_{\partial\Omega} [u(x)T_x \tilde{P}(x,y) - \tilde{P}(x,y)Tu(x)]d\Gamma(x) + \\ + \int_{\Omega} [\tilde{V}(x,y) + k(x)\tilde{P}(x,y)]u(x)d\Omega(x) = \int_{\Omega} \tilde{P}(x,y)f(x)d\Omega(x), \tag{11}$$

where,

$$\tilde{P}(x,y) = a(y)P(x,y) = \tfrac{1}{2\pi} \ln|x-y|,$$

$$\tilde{V}(x,y) = a(y)V(x,y) = \sum_{i=1}^{2} \tfrac{x_i - y_i}{2\pi|x-y|^2} \tfrac{\partial a(x)}{\partial x_i}$$

Differently from [18–22], the parametrix in identity (11) is the fundamental solution for the Laplace equation, which is much easier to implement in a unified code. Also, identity (11) can be used for formulating either a BDIE or BDIDE, with respect to u and its derivatives. Let us consider the two forms below.

3 Boundary-domain integral/integro-differential equations (BDIE/BDIDE)

3.1 Boundary-domain integral equation (BDIE)

Substituting the boundary conditions (2) and (3) into (11), introducing a new variable $t(x)=Tu(x)$ for the unknown normal velocity on $\partial_D\Omega$ and using Eq.(11) at $y \in \Omega \cup \partial\Omega$ reduces the BVP (1)-(3) to the following boundary-domain integral equation (BDIE) for $u(x)$ at $x \in \Omega \cup \partial_N\Omega$ and $t(x)$ at $x \in \partial_D\Omega$,

$$c^0(y)u(y) - \int_{\partial_N\Omega} u(x)T_x \tilde{P}(x,y)d\Gamma(x) + \int_{\partial_D\Omega} \tilde{P}(x,y)t(x)d\Gamma(x) + \\ + \int_{\Omega} [\tilde{V}(x,y) + k(x)\tilde{P}(x,y)]u(x)d\Omega(x) = \Psi^0(y), y \in \Omega \cup \partial\Omega \tag{12}$$

$$\Psi^0(y) := [c^o(y) - a(y)c(y)]\bar{u}(y) + \Psi(y), \tag{13}$$

$$\Psi(y) := \int\limits_{\partial_D\Omega} \bar{u}(x)T_x\tilde{P}(x,y)d\Gamma(x) - \int\limits_{\partial_N\Omega} \tilde{P}(x,y)\bar{t}(x)d\Gamma(x) + \int_\Omega \tilde{P}(x,y)f(x)d\Omega(x), \tag{14}$$

where $c^0(y)$ is

$$c^0(y) = \begin{cases} 0 & \text{if } y \in \partial_{\rm D}\Omega \\ a(y)c(y) & \text{if } y \in \Omega \cup \partial_{\rm N}\Omega \end{cases} \tag{15}$$

3.2 Boundary-domain integro-differential equation (BDIDE)

Using another approach, we can substitute the boundary conditions (2) and (3) into (11) but leave T as a differential operator acting on u on the Dirichlet boundary $\partial_D\Omega$ and use the following boundary-domain integro-differential equation (BDIDE) at $y \in \Omega \cup \partial_N\Omega$,

$$\begin{aligned} a(y)c(y)u(y) - \int\limits_{\partial_N\Omega} u(x)T_x\tilde{P}(x,y)d\Gamma(x) + \int\limits_{\partial_D\Omega} \tilde{P}(x,y)Tu(x)d\Gamma(x) + \\ + \int\limits_\Omega [\tilde{V}(x,y) + k(x)\tilde{P}(x,y)]u(x)d\Omega(x) = \Psi(y), y \in \Omega \cup \partial_N\Omega, \end{aligned} \tag{16}$$

where $\Psi(y)$ is given by Eq.(14). As we will see below, this approach can lead, after discretisation, to a system with a reduced number of linear algebraic equations.

4 Discretisation of the BDIE/BDIDE

4.1 Discretisation of the BDIE

Let us discretise the domain Ω into a mesh of triangular elements T_k, $k = 1, 2, ..., N$, $T_h \cap T_m = \emptyset$, $h \neq m$. Let J be the total number of nodes x^i, $i = 1, ..., J$, at the vertices of triangles, from which there are J_D nodes on $\partial_D\Omega$.

To obtain a system of linear algebraic equations from the BDIE (12), by the collocation method, we collocate at the nodes x^i, $i = 1, ..., J$ and substitute an interpolation of $u(x)$ of the form

$$u(x) \approx \sum_{\bar{\omega}_j \ni x} u(x^j)\Phi_j(x), \qquad \Phi_j(x) = \begin{cases} \phi_{kj}(x) & \text{if } \ x, x^j \in \bar{T}_k \\ 0 & \text{otherwise,} \end{cases} \tag{17}$$

where $\bar{\omega}_j$ is the support of $\Phi_j(x)$, which consists of all triangular elements that have x^j as a vertex; $\phi_{kj}(x)$ are the shape functions localized on an element T_k, and associated with the node x^j. For the triangular elements, $\phi_{kj}(x)$ can be chosen as piecewise linear functions. We can also use an interpolation of $t(x) = (Tu)(x^j)$ along boundary nodes belonging to $\bar{\omega}(x^j) \cap \partial_D\Omega$

$$t(x) = \sum_{x^j \in \bar{\omega}(x^j) \cap \partial_D\Omega} t(x^j)v_j(x), \ x \in \bar{\omega}(x^j) \cap \partial_D\Omega \tag{18}$$

Here, $v_j(x)$ are boundary shape functions, taken now as constant. Therefore, $v_j(x)$ will be equal 1 at $x_j \in \bar{\omega}(x^j) \cap \partial_D\Omega$ and $v_j(x) = 0$ if $x^j \notin \bar{\omega}(x^j) \cap \partial_D\Omega$. Substituting the interpolations (17) and (18) in BDIE (12) and applying the collocation method, we arrive at the following system of J linear algebraic equations for J unknowns $u(x^j)$, $x^j \in \Omega \cup \partial_N\Omega$ and $t(x^j) = (Tu)(x^j)$, $x^j \in \partial_D\Omega$,

$$c^0(x^i)u(x^i) + \sum_{x^j \in \Omega \cup \partial_N\Omega} M_{ij}u(x^j) + \sum_{x^j \in \Omega \cup \partial_N\Omega} DK_{ij}u(x^j) + \sum_{x^j \in \partial_D\Omega} M'_{ij}t(x^j) = \Psi^0(x^i) -$$
$$- \sum_{x^j \in \partial_D\Omega} M_{ij}\bar{u}(x^j) - \sum_{x^j \in \partial_D\Omega} DK_{ij}\bar{u}(x^j), x^i \in \Omega \cup \partial\Omega, \qquad i = 1, ..., J, \text{no sum in } i. \quad (19)$$

where $\Psi^0(x^i)$ is calculated from Eq. (13), and

$$\Psi(x^i) = \int\limits_{\bar{\omega}(x^i) \cap \partial_D\Omega} \bar{u}(x) T_x \tilde{P}(x, x^i) d\Gamma(x) - \int\limits_{\bar{\omega}(x^i) \cap \partial_N\Omega} \tilde{P}(x, x^i)\bar{t}(x) d\Gamma(x) + \int_\Omega \tilde{P}(x, x^i) f(x) d\Omega(x), \quad (20)$$

$$M_{ij} = - \int\limits_{\bar{\omega}(x^i) \cap \partial_N\Omega} \Phi_j(x) T_x \tilde{P}(x, x^i) d\Gamma(x) \quad (21)$$

$$M'_{ij} = \int\limits_{\bar{\omega}(x^i) \cap \partial_D\Omega} \tilde{P}(x, x^i) v_j(x) d\Gamma(x), \quad (22)$$

$$DK_{ij} = \int\limits_{\omega(x^i) \cap \Omega} \Phi_j(x)[\tilde{V}(x, x^i) + k(x)\tilde{P}(x, x^i)] d\Omega(x), \quad (23)$$

4.2 Discretisation of the BDIDE

To obtain a system of linear algebraic equations from the BDIDE (16) by the collocation method, we collocate at the nodes x^i, $i = 1, ...J$, arriving at a system of $J - J_D$ algebraic equations for $J - J_D$ unknowns $u(x^j)$, $x^j \in \Omega \cup \partial_N\Omega$. Substituting interpolation formulae (17) into the BDIDE (16) leads to the following system:

$$c(x^i)u(x^i) + \sum_{x^j \in \Omega \cup \partial_N\Omega} M''_{ij}u(x^j) + \sum_{x^j \in \Omega \cup \partial_N\Omega} DK_{ij}u(x^j) = \Psi(x^i) -$$
$$- \sum_{x^j \in \partial_D\Omega} M''_{ij}\bar{u}(x^j) - \sum_{x^j \in \partial_D\Omega} DK_{ij}\bar{u}(x^j), \quad x^i \in \Omega \cup \partial_N\Omega, \quad \text{no sum in } i, \quad (24)$$

where $\Psi(x^i)$ and DK_{ij} are given by Eqs. (20) and (23), respectively, and

$$M''_{ij} = \int\limits_{\bar{\omega}(x^i) \cap \partial_D\Omega} \tilde{P}(x, x^i) T\Phi_j(x) d\Gamma(x) - \int\limits_{\bar{\omega}(x^i) \cap \partial_N\Omega} \Phi_j(x) T_x \tilde{P}(x, x^i) d\Gamma(x) \quad (25)$$

5 Transformation of domain integrals to the boundary using RIM

In this section, the RIM [14, 15, 23, 26] is used to transform the domain integrals appearing in equations (12) and (16) into boundary integrals.

5.1 RIM formulation for domain integrals with known integrand

A domain integral with known integrand $f(x)$, $x = (x_1, x_2)$, can be transformed into an equivalent boundary integral by following the procedure given in detail in [14, 15, 23, 26]:

$$\int_{\Omega} f(x)d\Omega = \int_{\partial\Omega} \frac{1}{r^{\alpha}} \frac{\partial r}{\partial n} F(x)d\Gamma(x) \tag{26}$$

where

$$F(x) = \int_{0}^{r(x)} f(x) r^{\alpha} dr \tag{27}$$

In Eqs.(26) and (27), $\alpha = 1$ for the two-dimensional case and $\alpha = 2$ for the three-dimensional case. The symbol $r(x)$ means the variable r takes values on the boundary Γ, see Fig.(1).

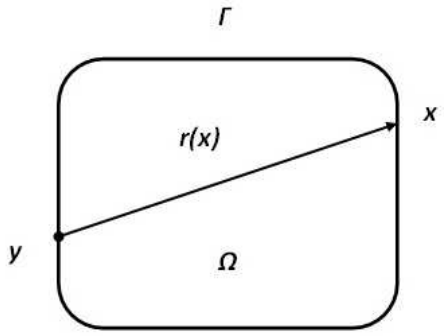

Fig. 1: Integration along radial direction r

The following remarks are important for the RIM:

• The most attractive feature of the RIM is that the transformation (26) is very simple and has similar forms for both 2D and 3D. It can remove various singularities appearing in domain integrals since r^{α} is included in the radial integral in Eq.(27).

In order to transform a domain integral to a boundary integral, the main task is to calculate the radial integral in Eq.(27), which can be done analytically for simple kernels. We have written a simple Matlab code for analytic integration of Eq.(27) which can integrate many given functions $f(x)$; however, for complicated functions, numerical integration techniques are required [14, 15]. Numerical integration can also be easily done in Matlab [26].

• In order to evaluate the radial integral in Eq.(27), the coordinates x_1, x_2 in $f(x)$ need to be expressed in terms of the distance r using:

$$x_i = y_i + r_{,i} r \qquad i = 1, 2 \tag{28}$$

where the quantities y_i and $r_{,i}$ are constant for the radial integral in Eq.(27), with $r_{,i} = \frac{x_i - y_i}{r}$.

• Following the idea presented in [24], we can introduce the change of variable:

$$r = t|x - y|, \quad t \in [0, 1] \tag{29}$$

and substitute the new transformation in the straight-line radial integral in Eq.(27), leading to:

$$F(x) = \int_0^1 f(y_1 + r_{,1}rt, y_2 + r_{,2}rt)r^2 t dt \tag{30}$$

The representation (30) makes it unnecessary to define a variable transformation as in [23] to treat the radial integral in Eq.(27), see Fig.1, adding an attractive feature to the RIM as Eq.(27) is now a pure boundary integral. Moreover, the star-shaped requirement for the integral in Eq.(27) can be relaxed as the straight path from the source point y to any field point x always exists [24].

5.1.1 Transformation of right-hand side domain integral to the boundary

Both Eq.(12) and Eq.(16) have domain integrals coming from the known function $f(x)$. The RIM can be directly used to convert these domain integrals to the boundary. This leads to

$$\int_\Omega \tilde{P}(x, y) f(x) d\Omega(x) = \int_{\partial\Omega} \frac{1}{r} \frac{\partial r}{\partial n} F(x) d\Gamma(x) \tag{31}$$

where

$$F(x) = \int_0^1 \tilde{P}(x, y) f(y_1 + r_{,1}rt, y_2 + r_{,2}rt)r^2 t dt \tag{32}$$

The integral in Eq.(32) can be calculated analytically for many different functions, and numerically without the need to define a transformation as in [14, 15]. Also, due to the radial integral in Eq.(32), the weak singularity coming from the fundamental solution is removed.

5.2 RIM formulation for domain integrals with unknown integrand

As the last domain integrals on the left-hand side of Eqs. (12) and (16) have the unknown function $u(x)$, the RIM in Eqs.(26) and (30) cannot be directly used. However, $u(x)$ can be approximated by radial basis functions [13,23,27]. We adopt an augmented radial basis function as discussed in [14, 23, 26–28].

Let us approximate the variation of $u(x)$ in the following way:

$$u(x) = \sum_{k=1}^{M} \alpha_k \phi_k(R) + c_1 x_1 + c_2 x_2 + c_3 \tag{33}$$

where $M = N_b + N_I$ and N_b, N_I are the number of boundary and interior nodes, respectively. Also, $R = \|x - a\|$ is the distance from the application point a to the field point x. Normally, the application points a consist of all boundary nodes and some selected interior nodes.

The constants c_1, c_2 and c_3 can be determined by the equilibrium constraints [28]:

$$\sum_{k=1}^{M} \alpha_k = \sum_{k=1}^{M} \alpha_k x_{1k} = \sum_{k=1}^{M} \alpha_k x_{2k} = 0 \tag{34}$$

The unknown coefficients α_k, c_1, c_2 and c_3 can be calculated by applying Eqs.(33) and (34) at the application points a, as discussed in detail in [26].

Substituting Eq.(33) into the last domain integral on the left-hand side of both Eqs.(12) and (16), we obtain:

$$\begin{aligned}\int_{\Omega} \{\tilde{V}(x,y) + k(x)\tilde{P}(x,y)\} u(x) d\Omega(x) = \sum_{k=1}^{M} \alpha_k \int_{\Omega} \{\tilde{V}(x,y) + k(x)\tilde{P}(x,y)\} \phi_k(R) d\Omega(x) + \\ + c_1 \int_{\Omega} \{\tilde{V}(x,y) + k(x)\tilde{P}(x,y)\} x_1 d\Omega(x) + c_2 \int_{\Omega} \{\tilde{V}(x,y) + k(x)\tilde{P}(x,y)\} x_2 d\Omega(x) + \\ + c_3 \int_{\Omega} \{\tilde{V}(x,y) + k(x)\tilde{P}(x,y)\} d\Omega(x)\end{aligned} \tag{35}$$

Let $r_{,1} = \frac{x_1 - y_1}{r}$ and $r_{,2} = \frac{x_2 - y_2}{r}$, then we can write:

$$\{\tilde{V}(x,y) + k(x)\tilde{P}(x,y)\} = \frac{1}{2\pi} \left(\frac{r_{,1}}{r} \frac{\partial a(x)}{\partial x_1} + \frac{r_{,2}}{r} \frac{\partial a(x)}{\partial x_2} + k(x)\tilde{P}(x,y) \right) \tag{36}$$

It is very important before applying the RIM using Eqs.(26) and (30), that the coordinates x_1 and x_2 appearing in Eqs.(35) and (36) are expressed in terms of the distance r using Eq.(28), see [23, 26].

Now, applying the RIM to each domain integral in Eq.(35) leads to

$$\int_{\Omega} \{\tilde{V}(x,y) + k(x)\tilde{P}(x,y)\} u(x) d\Omega(x) = \int_{\partial\Omega} h(x) d\Gamma(x)$$

and

$$\begin{aligned}\int_{\partial\Omega} h(x) d\Gamma(x) = \sum_{k=1}^{M} \alpha_k \int_{\partial\Omega} \frac{1}{r} \frac{\partial r}{\partial n} F1(x) d\Gamma(x) + c_1 \int_{\partial\Omega} \frac{1}{r} \frac{\partial r}{\partial n} F2(x) d\Gamma(x) + \\ + c_2 \int_{\partial\Omega} \frac{1}{r} \frac{\partial r}{\partial n} F3(x) d\Gamma(x) + c_3 \int_{\partial\Omega} \frac{1}{r} \frac{\partial r}{\partial n} F4(x) d\Gamma(x)\end{aligned} \tag{37}$$

where

$$F1(x) = \int_0^1 \{\tilde{V}(x,y) + k(y_1 + r_{,1}rt, y_2 + r_{,2}rt)\tilde{P}(x,y)\}\phi(R)r^2 tdt \tag{38a}$$

$$F2(x) = \int_0^1 \{\tilde{V}(x,y) + k(y_1 + r_{,1}rt, y_2 + r_{,2}rt)\tilde{P}(x,y)\}(y_1 + r_{,1}rt)r^2 tdt \tag{38b}$$

$$F3(x) = \int_0^1 \{\tilde{V}(x,y) + k(y_1 + r_{,1}rt, y_2 + r_{,2}rt)\tilde{P}(x,y)\}(y_2 + r_{,2}rt)r^2 tdt \tag{38c}$$

$$F4(x) = \int_0^1 \{\tilde{V}(x,y) + k(y_1 + r_{,1}rt, y_2 + r_{,2}rt)\tilde{P}(x,y)\}r^2 tdt \tag{38d}$$

The four integrals in Eq.(38) can be easily integrated numerically in Matlab. Since $\phi(R)$ in Eq.(38a) is a function of the distance R, see Table 1, $\phi(R)$ needs to be expressed in terms of the distance r. Gao [14,15], referring to Fig. 2, defined three vectors ay with length $\bar{R}$, ax with length R and yx with length r.

From elementary calculus, we have the following identity:

$$ax = ay + yx$$

Therefore,

$$(ax)^2 = (ay + yx)(ay + yx) = (ay)^2 + 2ay \cdot yx + (yx)^2$$

Then,

$$R = \sqrt{\bar{R}^2 + sr + r^2} \tag{39}$$

where $s = 2\left(\frac{(x-y)(y-a)}{r}\right)$.

Tab. 1: Commonly used radial basis functions $\phi(R)$

R	$R+1$	R^3	$1+R^2+R^3$	$R^2 \log R$

In this paper, we use a simpler procedure that leads to exactly the same results as in Eq.(39), in which we express $\phi(R) = R$ (for simplicity we choose $\phi(R) = R$ below but $\phi(R) = R^3$ will be adopted in all test examples) in terms of r as follows:

$$R = \sqrt{(a_1 - x_1)^2 + (a_2 - x_2)^2}$$

where a_1 and a_2 are the coordinates of the application point. Then, using Eqs.(28) and (29), we get

$$R = \sqrt{(a_1 - (y_1 + r_{,1}rt))^2 + (a_2 - (y_2 + r_{,2}rt))^2}$$

It is important to notice that the integrands in Eq.(38) are all regular as the term r^2 cancels the singularity of the term $\tilde{V}(x,y)$ defined in Eq.(36).

After numerical integration, the unknown coefficients $\alpha_k, k = 1.....M$, c_1, c_2 and c_3, can be calculated following the procedures discussed in [26].

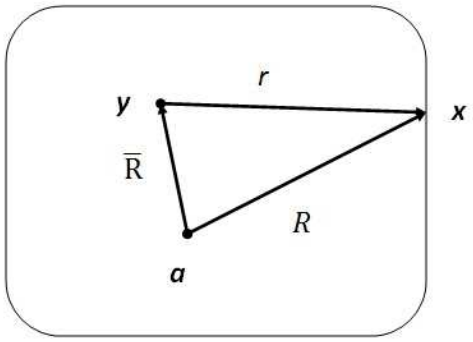

Fig. 2: Relationship between distances

6 The radial integration boundary integral and integro-differential equations (RIBIE/RIBIDE)

Eqs.(31)-(32) and (37)-(38) can now be substituted in both BDIE in Eq.(12) and BDIDE in Eq.(16), leading to the expressions in the next subsections.

6.1 Radial integration boundary integral equation (RIBIE)

$$c^0(y)u(y) - \int\limits_{\partial_N\Omega} u(x)T_x\tilde{P}(x,y)d\Gamma(x) + \int\limits_{\partial_D\Omega} \tilde{P}(x,y)t(x)d\Gamma(x) + \\ + \int\limits_{\partial\Omega} h(x)d\Gamma(x) = \Psi^0(y), y \in \Omega \cup \partial\Omega \tag{40}$$

$$\Psi^0(y) := [c^o(y) - a(y)c(y)]\bar{u}(y) + \tilde{\Psi}(y), \tag{41}$$

$$\tilde{\Psi}(y) := \int\limits_{\partial_D\Omega} \bar{u}(x)T_x\tilde{P}(x,y)d\Gamma(x) - \int\limits_{\partial_N\Omega} \tilde{P}(x,y)\bar{t}(x)d\Gamma(x) + \int\limits_{\partial\Omega} \frac{1}{r}\frac{\partial r}{\partial n}F(x)d\Gamma(x) \tag{42}$$

where $c^0(y)$, $F(x)$ and $\int\limits_{\partial\Omega} h(x)d\Gamma(x)$ are given in Eqs.(15), (32) and (37)-(38), respectively.

6.2 Radial integration boundary integro-differential equation (RIBIDE)

$$a(y)c(y)u(y) - \int\limits_{\partial_N\Omega} u(x)T_x\tilde{P}(x,y)d\Gamma(x) + \int\limits_{\partial_D\Omega} \tilde{P}(x,y)Tu(x)d\Gamma(x) + \\ + \int\limits_{\partial\Omega} h(x)d\Gamma(x) = \tilde{\Psi}(y), y \in \Omega \cup \partial_N\Omega \tag{43}$$

where $\int_{\partial\Omega} h(x)d\Gamma(x)$ and $\tilde{\Psi}(y)$ are given in Eqs.(37)-(38) and (42), respectively.

It can be clearly seen from both RIBIE in Eq.(40) and RIBIDE in Eq.(43) that all integrations are now carried out only on the boundary, with no domain integrals.

7 Discretisation of the radial integration boundary integral and integro-differential equations (RIBIE/RIBIDE)

7.1 Discretisation of the RIBIE

The RIBIE formulation employs mixed boundary elements with linear u and constant t to avoid the discontinuities of t at corner points. In this case, collocation was taken at the end points of each boundary element, since our previous research has shown that end-node collocation generally provides higher accuracy than mid-node collocation [20, 26].

Let J be the total number of nodes x^i, $i = 1, ..., J$, at the end points of elements, from which there are J_D nodes on $\partial_D\Omega$. Thus, the values of u at any point on the element can be defined in terms of their nodal values and two linear interpolation functions $\Psi^1(t)$ and $\Psi^2(t)$, see e.g. [4]:

$$\Psi^1(t) = \frac{1}{2}(1-t);\ \Psi^2(t) = \frac{1}{2}(1+t) \tag{44}$$

where t is the reference coordinate along the element with values -1, +1, at the end points.

To obtain a system of linear algebraic equations from the RIBIE (40), we collocate at the nodes x^i, $i = 1, ..., J$. We can also use an interpolation of $t(x) = (Tu)(x^j)$ along boundary nodes belonging to $x^j \in \partial_D\Omega$

$$t(x) = \sum_{x^j \in \partial_D\Omega} t(x^j)v_j(x),\ x \in \partial_D\Omega \tag{45}$$

Here, $v_j(x)$ are boundary shape functions, taken now as constant. Therefore, $v_j(x)$ will be equal to 1 at $x^j \in \partial_D\Omega$ and $v_j(x) = 0$ if $x^j \notin \partial_D\Omega$. Substituting the interpolations (44) and (45) in the RIBIE (40) and applying the collocation method, we arrive at the following system of J linear algebraic equations for J unknowns $u(x^j)$, $x^j \in \Omega \cup \partial_N\Omega$ and $t(x^j) = (Tu)(x^j)$, $x^j \in \partial_D\Omega$,

$$c^0(x^i)u(x^i) + \sum_{x^j \in \Omega \cup \partial_N\Omega} K_{ij}u(x^j) + \sum_{x^j \in \partial_D\Omega} Q'_{ij}t(x^j) = \Psi^0(x^i) - \sum_{x^j \in \partial_D\Omega} K_{ij}\bar{u}(x^j),$$
$$x^i \in \Omega \cup \partial\Omega, \qquad i = 1, ..., J, \text{no sum in } i, \tag{46}$$

where $\Psi^0(x^i)$ is calculated from Eq.(14), and

$$\tilde{\Psi}(x^i) = \int_{\partial_D\Omega} \bar{u}(x)T_x\tilde{P}(x, x^i)d\Gamma(x) - \int_{\partial_N\Omega} \tilde{P}(x, x^i)\bar{t}(x)d\Gamma(x) + \int_{\partial\Omega} \frac{1}{r}\frac{\partial r}{\partial n}F(x)d\Gamma(x) \tag{47}$$

$$K_{ij} = \int_{\partial\Omega} h(x)d\Gamma(x) - \int_{\partial_N\Omega} [\Psi^1, \Psi^2]T_x\tilde{P}(x, x^i)d\Gamma(x) \tag{48}$$

$$Q'_{ij} = \int_{\partial_D\Omega} \tilde{P}(x, x^i)v_j(x)d\Gamma(x) \tag{49}$$

where $F(x)$ is given in Eq.(32) and $\int_{\partial\Omega} h(x)d\Gamma(x)$ is given in Eqs.(37)-(38)

7.2 Discretisation of the RIBIDE

To obtain a system of linear algebraic equations from the RIBIDE (43), we collocate at the nodes x^i, $i = 1, ...J$, and substitute an interpolation of $u(x)$ of the form

$$u(x) \approx \sum_{S_j \ni x} u(x^j)\Phi_j(x), \qquad \Phi_j(x) = \begin{cases} \phi_{kj}(x) & \text{if } \ x, x^j \in \bar{T}_k \\ 0 & \text{otherwise,} \end{cases} \tag{50}$$

where S_j in this case is the set of collocation points in $\partial_D\Omega$ and some selected interior nodes near the boundary segments; $\phi_{kj}(x)$ are the shape functions which can be constructed from the distance between the two end nodes of each segments and the selected interior nodes, and associated with the node x^j. In this work, $\phi_{kj}(x)$ are chosen as piecewise linear functions.

We then arrive at a system of $J - J_D$ algebraic equations for $J - J_D$ unknowns $u(x^j)$, $x^j \in \Omega \cup \partial_N\Omega$. Substituting interpolation formulae (50) into the RIBIDE (43) leads to the following system of equations:

$$a(x^i)c(x^i)u(x^i) + \sum_{x^j \in \Omega \cup \partial_N\Omega} K'_{ij}u(x^j) = \tilde{\Psi}(x^i) - \sum_{x^j \in \partial_D\Omega} K'_{ij}\bar{u}(x^j), \qquad x^i \in \Omega \cup \partial_N\Omega, \ \text{ no sum in } i, \tag{51}$$

where

$$K'_{ij} = K_{ij} + \int_{\partial_D\Omega} \tilde{P}(x, x^i)T\Phi_j(x)d\Gamma(x) \tag{52}$$

and $\tilde{\Psi}(x^i)$ and K_{ij} are given in Eqs.(47) and (48), respectively.

The calculation of the integral in Eq.(52) is presented in detail in [26]. The advantages of the RIBIDE technique are that the only boundary variables are those of u along Neumann boundaries, as there is no need for collocation along Dirichlet boundaries. Thus, the problem caused by the discontinuity of the normal derivative at corner points is avoided. Second, the system of linear equations is smaller than the one for RIBIE. This feature will save memory and computational time when we apply the RIBIDE for practical problems. Finally, the assembly of matrix A and vector b is much easier than in the RIBIE, as discussed in [20].

8 Numerical results

In this section, we shall examine some test examples to assess the performance of the RIBIDE/RIBIE formulations for the non-homogeneous Helmholtz equation with variable coefficients for three cases. Firstly, when the parameter $a(x)$ is variable and the wave number k is constant. Secondly, when the parameter $a(x)$ is constant and the wave number $k(x)$ is variable. Thirdly, when both the parameter $a(x)$ and the wave number $k(x)$ are variable. For comparison, the problems are also computed using both BDIDE and BDIE.

We applied the RIBIDE/RIBIE and BDIE/BDIDE methods to some test problems on a square domain, for which an exact analytical solution, u_{exact}, is available. Computer programs were developed by using Matlab. The exact solutions of the problems range from linear to cubic, and will be used to verify the convergence of the numerical solutions. Moreover, $\phi(R) = R^3$ is adopted in the test examples. The total number of nodes is 81 (32 on the boundary plus 49 in the interior). Also, the top and bottom sides of the plates for all tests examples have prescribed acoustic pressure u (Dirichlet boundary conditions), while the left and right are imposed with normal velocity t (Neumann boundary conditions). The relative error and Root Mean Square

(RMS) error are calculated to check the convergence of the proposed methods:

$$r(J) = \frac{\max\limits_{1\le j\le J} \left| u_{approx}(x^j) - u_{exact}(x^j) \right|}{\max\limits_{1\le j\le J} \left| u_{exact}(x^j) \right|} \tag{53}$$

$$RMS(J) = \left(\frac{\sum_{j=1}^{J} (u_{approx,j} - u_{exact,j})^2}{\sum_{j=1}^{J} u_{exact,j}^2} \right)^{1/2}, \tag{54}$$

where u_{approx} is the numerical solution and J is the number of nodes in the computational mesh. These errors have been calculated for J= 25, 81, 289 and 1089 in all test examples.

8.1 Numerical results for non-homogeneous Helmholtz equation with variable $a(x)$ and constant k

8.1.1 Test 1:

Square domain $\bar{\Omega} = \{(x_1, x_2) : 1 \le x_1, x_2 \le 2\}$, where $k(x) = 1$, for $x \in \bar{\Omega}$, $a(x) = x_1^2 + x_2^2$, $f(x) = 9(x_1^2 + x_2^2)$ and the boundary conditions:

$\bar{u}(x) = 1 + x_1^2$, for $x_2 = 1$; $1 \le x_1 \le 2$,

$\bar{u}(x) = 4 + x_1^2$, for $x_2 = 2$; $1 \le x_1 \le 2$,

$\bar{t}(x) = 2(x_1^2 + x_2^2)(x_1 n_1(x) + x_2 n_2(x))$, for $x_1 = 1$ or $x_1 = 2$; $1 \le x_2 \le 2$

where $n_1(x)$ and $n_2(x)$ are the components of the external normal vector $n(x)$. The exact solution for this problem is $u_{exact}(x) = x_1^2 + x_2^2$, $x \in \bar{\Omega}$.

Table 2 lists the computed values of $u(x)$ along the middle line of the plate using RIBIDE, RIBIE, BDIDE and BDIE, Figs. 3 and 4 plot the relative and RMS errors for RIBIDE and RIBIE, respectively, while Fig.5 shows the variation of $u(x)$ along the line $x_2 = 2.875$.

Tab. 2: Computed acoustic pressure along line of $x_2 = 1.5$

x_1	BDIDE	RIBIDE	BDIE	RIBIE	Exact
1	3.23904254	3.27576532	3.25001788	3.25005523	3.25000000
1.125	3.50524145	3.53417482	3.51695736	3.51663265	3.51562500
1.25	3.80173933	3.82657272	3.81393990	3.81329415	3.81250000
1.375	4.12971330	4.14846598	4.14223153	4.14130378	4.14062500
1.5	4.48916298	4.50394266	4.50185631	4.50065229	4.50000000
1.625	4.88007916	4.88811964	4.89283775	4.89134235	4.89062500
1.750	5.30243537	5.30636671	5.31520029	5.31335853	5.31250000
1.875	5.75620027	5.75461679	5.76895964	5.76669239	5.76562500
2	6.23998789	6.23825471	6.25274089	6.24995223	6.25000000

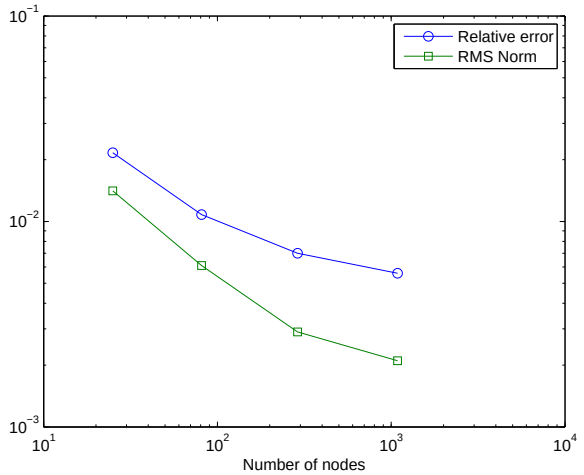

Fig. 3: Relative and RMS errors for RIBIDE method for test 1

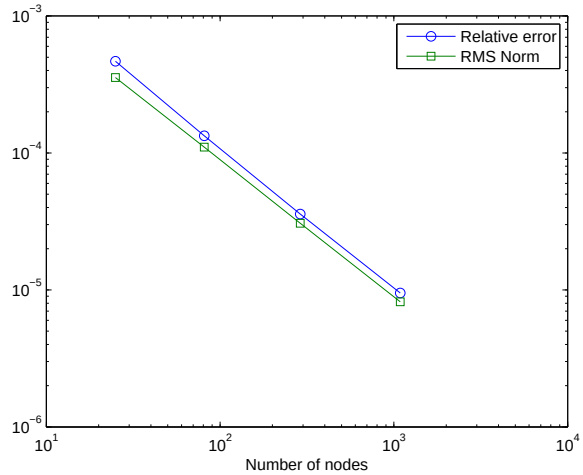

Fig. 4: Relative and RMS errors for RIBIE method for test 1

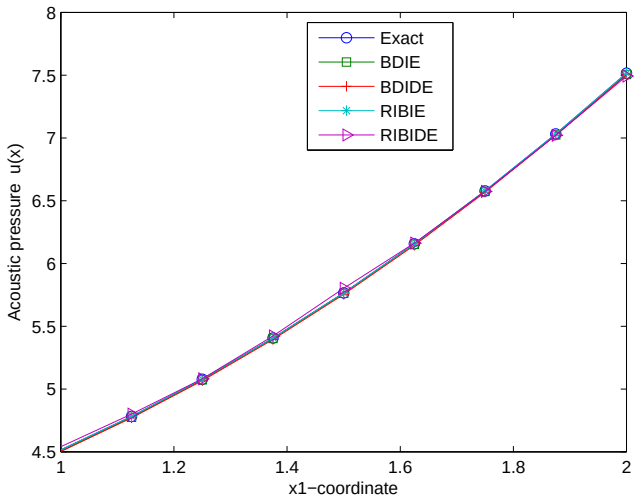

Fig. 5: Acoustic pressure distribution along the line $x_2 = 1.875$

8.1.2 Test 2 :

Square domain $\bar{\Omega} = \{(x_1, x_2) : 2 \leq x_1, x_2 \leq 3\}$, where $k(x) = 1$, for $x \in \bar{\Omega}$, $a(x) = \exp(x_1 + x_2)$, $f(x) = \exp(x_1 + x_2)(6x_1 + 3x_1^2 + 6x_2 + 3x_2^2) + x_1^3 + x_2^3$ and the boundary conditions:

$\bar{u}(x) = 8 + x_1^3$, for $x_2 = 2$; $2 \leq x_1 \leq 3$,

$\bar{u}(x) = 27 + x_1^3$, for $x_2 = 3$; $2 \leq x_1 \leq 3$,

$\bar{t}(x) = \exp(x_1 + x_2)(3x_1^2 n_1(x) + 3x_2^2 n_2(x))$, for $x_1 = 2$ or $x_1 = 3$; $2 \leq x_2 \leq 3$

The exact solution for this problem is $u_{exact}(x) = x_1^3 + x_2^3$, $x \in \bar{\Omega}$.

Table 3 lists the computed values of $u(x)$ along the middle line of the plate using RIBIDE, RIBIE, BDIDE and BDIE, Figs. 6 and 7 plot the relative and RMS errors for RIBIDE and RIBIE, respectively, while Fig.8 shows the variation of $u(x)$ along the line $x_2 = 2.875$.

Tab. 3: Computed acoustic pressure along line $x_2 = 2.5$

x_1	BDIDE	RIBIDE	BDIE	RIBIE	Exact
2	23.54227795	24.08753950	23.60035796	23.62472805	23.62500000
2.125	25.14006793	25.58360246	25.20769297	25.22737334	25.22070313
2.25	26.93069620	27.28226866	27.00518929	27.02088546	27.01562500
2.375	28.93457973	29.20969252	29.01338124	29.02608159	29.02148438
2.5	31.16338664	31.36617250	31.24439482	31.25465503	31.25000000
2.625	33.62869650	33.75998894	33.71028780	33.71823012	33.71289063
2.750	36.34196670	36.40889990	36.42304776	36.42847247	36.42187500
2.875	39.31462484	39.31873001	39.39451701	39.39688883	39.38867188
3	42.54759473	42.52953357	42.62601667	42.62475880	42.62500000

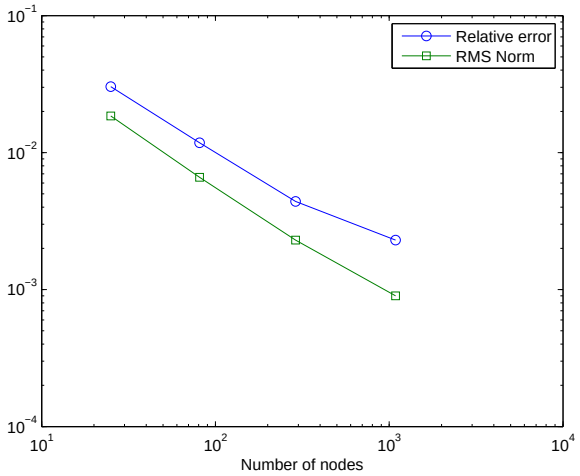

Fig. 6: Relative and RMS errors for RIBIDE method for test 2

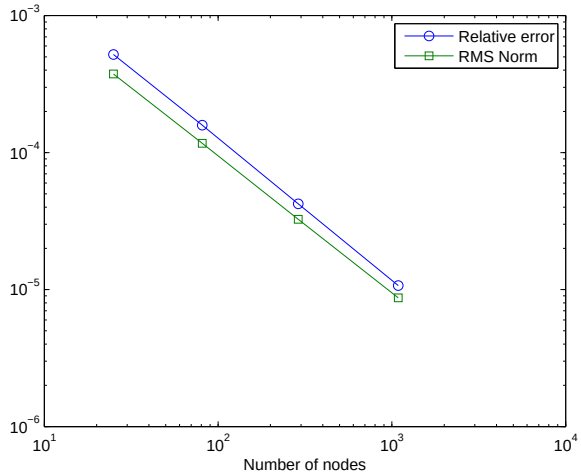

Fig. 7: Relative and RMS errors for RIBIE method for test 2

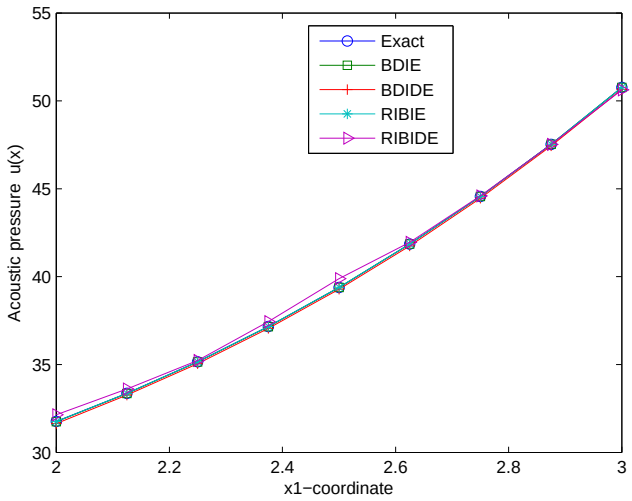

Fig. 8: Acoustic pressure distribution along the line $x_2 = 2.875$

It can be seen from Tables 2-3 and Figs. 5 and 8 that both the RIBIE and RIBIDE methods are able to generate accurate solutions in good agreement with BDIE and BDIDE results.

8.2 Numerical results for non-homogeneous Helmholtz equation with constant $a(x)$ and variable $k(x)$

In this case, when the parameter $a(x)$ is constant, the remainder $V(x, y)$ in Eq.(10) will be zero. Therefore, the parametrix in Eq.(9) is exactly the same as the fundamental solution for the Laplace equation.

8.2.1 Test 3 :

Square domain $\bar{\Omega} = \{(x_1, x_2) : 0 \leq x_1, x_2 \leq 1\}$, where $k(x) = x_1^3 + x_2^3$, for $x \in \bar{\Omega}$, $a(x) = 1$, $f(x) = (x_1^3 + x_2^3)(x_1 + x_2)$ and the boundary conditions:

$\bar{u}(x) = x_1$, for $x_2 = 0$; $0 \leq x_1 \leq 1$

$\bar{u}(x) = 1 + x_1$, for $x_2 = 1$; $0 \leq x_1 \leq 1$

$\bar{t}(x) = n_1(x) + n_2(x)$, for $x_1 = 0$ or $x_1 = 1$; $0 \leq x_2 \leq 1$

The exact solution for this problem is $u_{exact}(x) = x_1 + x_2$, $x \in \bar{\Omega}$.

Table 4 lists the computed values of $u(x)$ along the middle line of the plate using RIBIDE, RIBIE, BDIDE and BDIE, Figs. 9 and 10 plot the relative and RMS errors for RIBIDE and RIBIE, respectively, while Fig.11 shows the variation of $u(x)$ along the line $x_2 = 0.875$.

Tab. 4: Computed acoustic pressure along line $x_2 = 0.5$

x_1	BDIDE	RIBIDE	BDIE	RIBIE	Exact
0	0.50001354	0.49808573	0.50001417	0.50001295	0.50000000
0.125	0.62500238	0.62295805	0.62500297	0.62499982	0.62500000
0.25	0.75000135	0.74742745	0.75000181	0.74999816	0.75000000
0.375	0.87500056	0.87244433	0.87500085	0.87499711	0.87500000
0.5	0.99999989	0.99766609	0.99999998	0.99999501	1.00000000
0.625	1.12499922	1.12187828	1.12499910	1.12499501	1.12500000
0.750	1.24999839	1.24604751	1.24999810	1.24999412	1.25000000
0.875	1.37499729	1.37172154	1.37499688	1.37499191	1.37500000
1	1.49998607	1.49586330	1.49998561	1.49998264	1.50000000

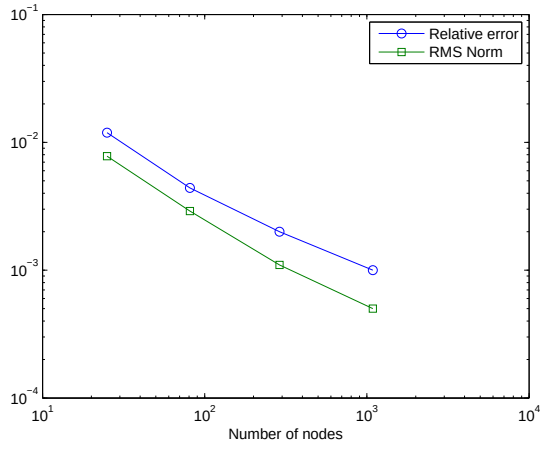

Fig. 9: Relative and RMS errors for RIBIDE method for test 3

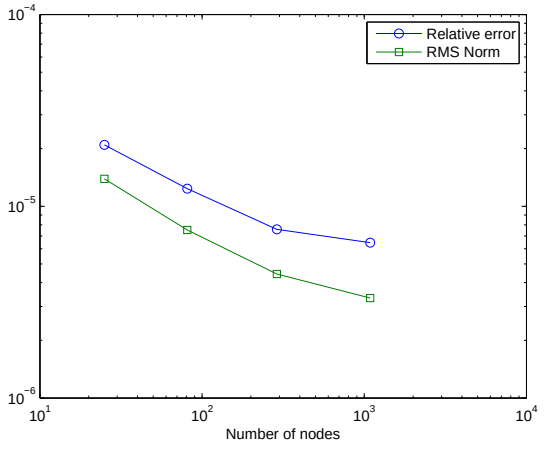

Fig. 10: Relative and RMS errors for RIBIE method for test 3

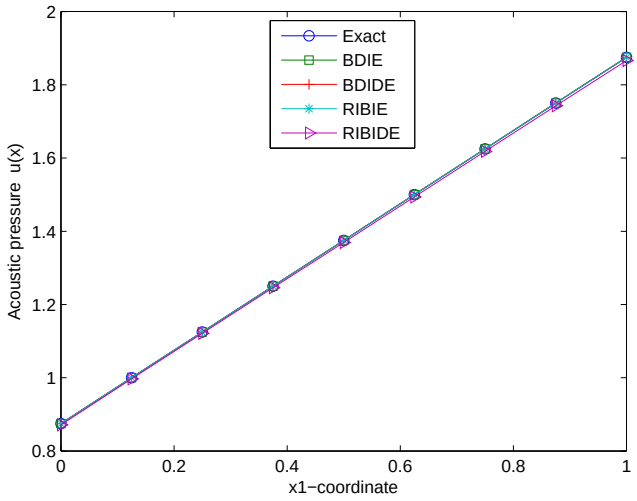

Fig. 11: Acoustic pressure distribution along the line $x_2 = 0.875$

8.2.2 Test 4 :

Square domain $\bar{\Omega} = \{(x_1, x_2) : 2 \leq x_1, x_2 \leq 3\}$, where $k(x) = \cos(x_1) + \cos(x_2)$, for $x \in \bar{\Omega}$, $a(x) = 1$, $f(x) = (\cos(x_1) + \cos(x_2))(x_1 + x_2)$ and the boundary conditions:

$\bar{u}(x) = 2 + x_1$, for $x_2 = 2$; $2 \leq x_1 \leq 3$

$\bar{u}(x) = 3 + x_1$, for $x_2 = 3$; $2 \leq x_1 \leq 3$

$\bar{t}(x) = n_1(x) + n_2(x)$, for $x_1 = 2$ or $x_1 = 3$; $2 \leq x_2 \leq 3$

The exact solution for this problem is $u_{exact}(x) = x_1 + x_2$, $x \in \bar{\Omega}$.

Table 5 lists the computed values of $u(x)$ along the middle line of the plate using RIBIDE, RIBIE, BDIDE and BDIE, Figs. 12 and 13 plot the relative and RMS errors for RIBIDE and RIBIE, respectively, while Fig.14 shows the variation of $u(x)$ along the line $x_2 = 2.875$.

Tab. 5: Computed acoustic pressure along line of $x_2 = 2.5$

x_1	BDIDE	RIBIDE	BDIE	RIBIE	Exact
2	4.50001317	4.50314478	4.50001361	4.50001702	4.50000000
2.125	4.62500210	4.63140975	4.62500249	4.62500705	4.62500000
2.25	4.75000120	4.76005830	4.75000149	4.75000504	4.75000000
2.375	4.87500055	4.88111739	4.87500069	4.87500317	4.87500000
2.5	5.00000005	5.00489097	4.99999999	5.00000137	5.00000000
2.625	5.12499955	5.13117889	5.12499932	5.12500185	5.12500000
2.750	5.24999893	5.25665463	5.24999854	5.25000135	5.25000000
2.875	5.37499806	5.37992272	5.37499757	5.37500057	5.37500000
3	5.49998701	5.49941772	5.49998648	5.49998770	5.50000000

From Tables 4-5 and Figs. 11 and 14, it is clear that both the RIBIE and RIBIDE methods are able to generate accurate solutions in good agreement with BDIE and BDIDE results.

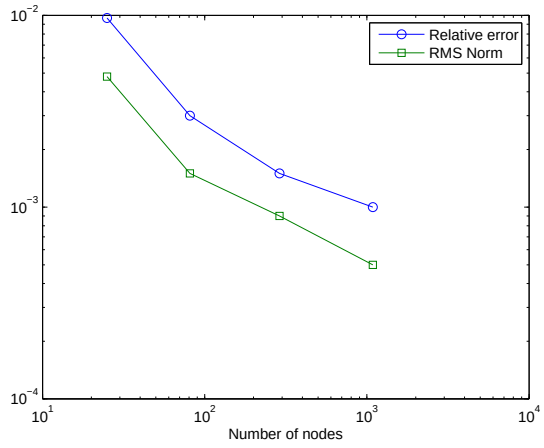

Fig. 12: Relative and RMS errors for RIBIDE method for test 4

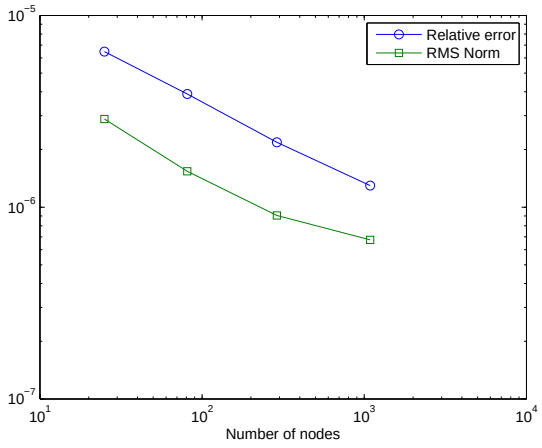

Fig. 13: Relative and RMS errors for RIBIE method for test 4

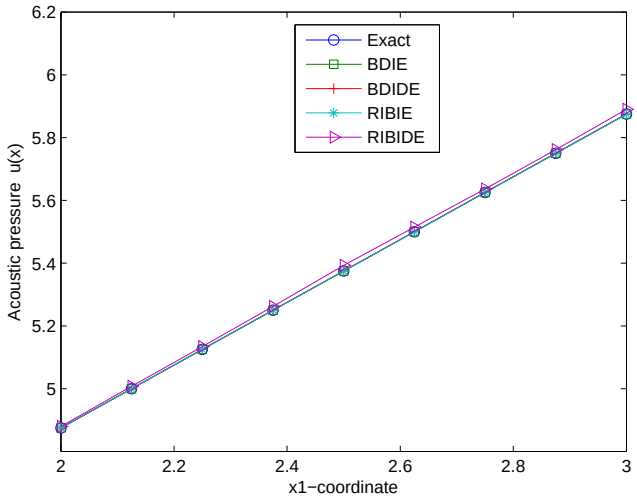

Fig. 14: Acoustic pressure distribution along the line $x_2 = 2.875$

8.3 Numerical results for non-homogeneous Helmholtz equation with both $a(x)$ and $k(x)$ variable

In this final case, when both the material parameter $a(x)$ and wave number $k(x)$ are variable, the parametrix in Eq.(9) is adopted. Let us consider some test examples to assess the accuracy of the RIBIDE/RIBIE and BDIDE/BDIE methods.

8.3.1 Test 5 :

Square domain $\bar{\Omega} = \{(x_1, x_2) : 1 \leq x_1, x_2 \leq 2\}$, where $k(x) = x_1 + x_2$, for $x \in \bar{\Omega}$, $a(x) = \exp(x_1 + x_2)$, $f(x) = 2(\exp(x_1 + x_2)) + (x_1 + x_2)^2$ and the boundary conditions:

$\bar{u}(x) = 1 + x_1$, for $x_2 = 1$; $1 \leq x_1 \leq 2$

$\bar{u}(x) = 2 + x_1$, for $x_2 = 2$; $1 \leq x_1 \leq 2$

$\bar{t}(x) = (\exp(x_1 + x_2))(n_1(x) + n_2(x))$, for $x_1 = 1$ or $x_1 = 2$; $1 \leq x_2 \leq 2$

The exact solution for this problem is $u_{exact}(x) = x_1 + x_2$, $x \in \bar{\Omega}$.

Tab. 6: Computed acoustic pressure along line of $x_2 = 1.5$

x_1	BDIDE	RIBIDE	BDIE	RIBIE	Exact
1	2.50000827	2.53200759	2.49975098	2.49997915	2.50000000
1.125	2.62499815	2.65179178	2.62485102	2.62497797	2.62500000
1.25	2.74999800	2.77092058	2.74992766	2.74998578	2.75000000
1.375	2.87499777	2.89109656	2.87499185	2.87499340	2.87500000
1.5	2.99999737	3.01111090	3.00004969	3.00000009	3.00000000
1.625	3.12499670	3.13157705	3.12510806	3.12500611	3.12500000
1.750	3.24999566	3.25284233	3.25017286	3.25001177	3.25000000
1.875	3.37499422	3.37410114	3.37524777	3.37501589	3.37500000
2	3.49998273	3.49815802	3.50034354	3.50000900	3.50000000

Table 6 lists the computed values of $u(x)$ along the middle line of the plate using RIBIDE, RIBIE, BDIDE and BDIE, Figs. 15 and 16 plot the relative and RMS errors for RIBIDE and RIBIE, respectively, while Fig.17 shows the variation of $u(x)$ along the line $x_2 = 1.875$.

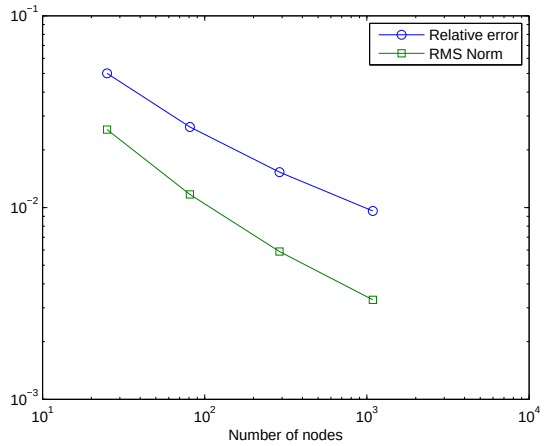

Fig. 15: Relative and RMS errors for RIBIDE method for test 5

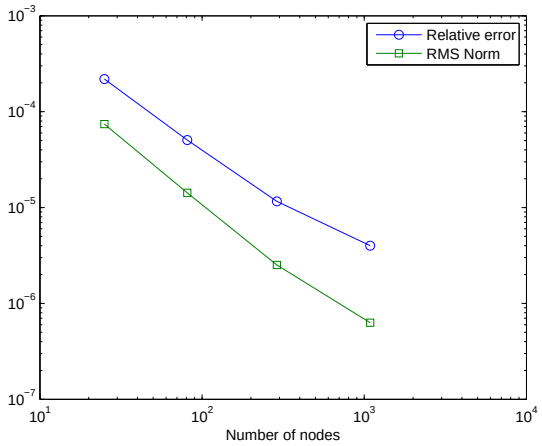

Fig. 16: Relative and RMS errors for RIBIE method for test 5

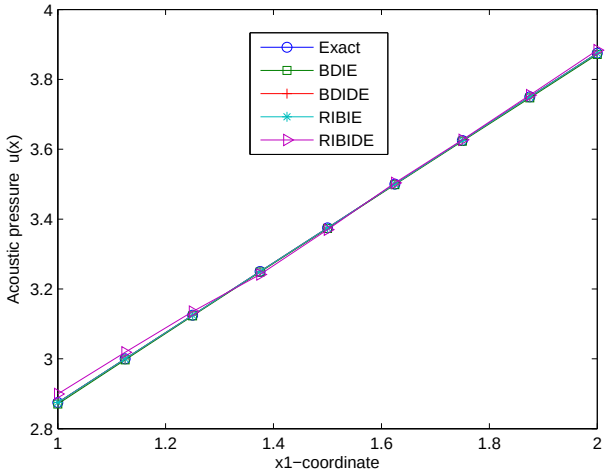

Fig. 17: Acoustic pressure distribution along the line $x_2 = 1.875$

8.3.2 Test 6 :

Square domain $\bar{\Omega} = \{(x_1, x_2) : 1 \leq x_1, x_2 \leq 2\}$, where $k(x) = \sin(x_1) + \sin(x_2)$, for $x \in \bar{\Omega}$, $a(x) = \exp(x_1 + x_2)$, $f(x) = (2(\exp(x_1 + x_2))(2 + x_1 + x_2)) + (\sin(x_1) + \sin(x_2))(x_1^2 + x_2^2)$ and the boundary conditions:

$\bar{u}(x) = 1 + x_1$, for $x_2 = 1$; $1 \leq x_1 \leq 2$

$\bar{u}(x) = 2 + x_1$, for $x_2 = 2$; $1 \leq x_1 \leq 2$

$\bar{t}(x) = 2(\exp(x_1 + x_2))(x_1 n_1(x) + x_2 n_2(x))$, for $x_1 = 1$ or $x_1 = 2$; $1 \leq x_2 \leq 2$

The exact solution for this problem is $u_{exact}(x) = x_1^2 + x_2^2$, $x \in \bar{\Omega}$.

Table 7 lists the computed values of $u(x)$ along the middle line of the plate using RIBIDE, RIBIE, BDIDE and BDIE, Figs. 18 and 19 plot the relative and RMS errors for RIBIDE and RIBIE, respectively, while Fig.20 shows the variation of $u(x)$ along the line $x_2 = 1.875$.

Tab. 7: Computed acoustic pressure along line of $x_2 = 1.5$

x_1	BDIDE	RIBIDE	BDIE	RIBIE	Exact
1	3.23907298	3.32246311	3.24875134	3.24996383	3.25000000
1.125	3.50510973	3.57286266	3.51593634	3.51652295	3.51562500
1.25	3.80153097	3.85513479	3.81314959	3.81320922	3.81250000
1.375	4.12948095	4.17133413	4.14165412	4.14125138	4.14062500
1.5	4.48895221	4.51957143	4.50149612	4.50063760	4.50000000
1.625	4.87992777	4.89980552	4.89272494	4.89135856	4.89062500
1.750	5.30237464	5.31223044	5.31538789	5.31340484	5.31250000
1.875	5.75625542	5.75675965	5.76951472	5.76675756	5.76562500
2	6.24013358	6.23692919	6.25374388	6.25000002	6.25000000

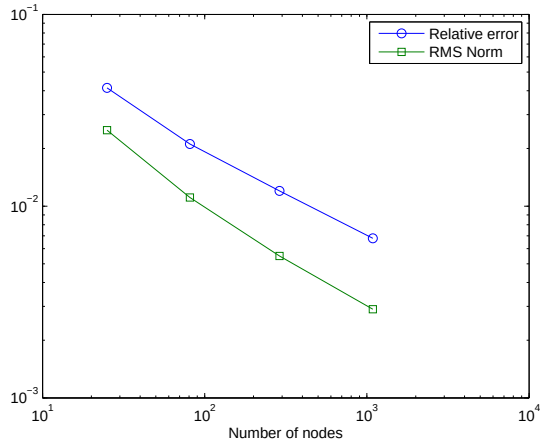

Fig. 18: Relative and RMS errors for RIBIDE method for test 6

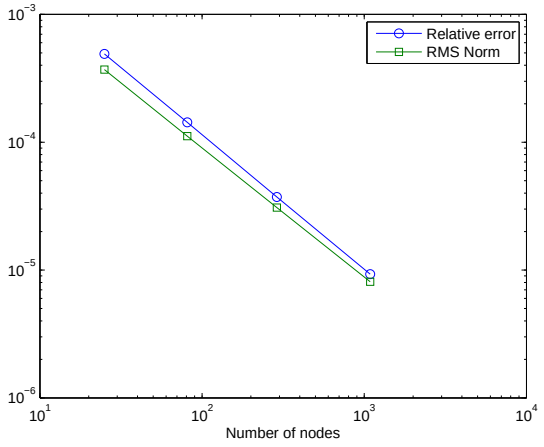

Fig. 19: Relative and RMS errors for RIBIE method for test 6

It can be seen from Tables 6-7 and Figs.17 and 20 that both the RIBIE and RIBIDE methods are able to generate accurate solutions in good agreement with the BDIE and BDIDE results. It is important to point out that the numerical integration of the RIM in Matlab is very fast and can save a substantial amount of computational time in comparison to both BDIDE and BDIE. It is noticed that the RIBIE produces better results than RIBIDE in all tests. Moreover, the relative and RMS errors in tests 1-7 show that both the RIBIE and RIBIDE methods are convergent with mesh refinement and, in general, the RMS error is lower than the relative error, as expected.

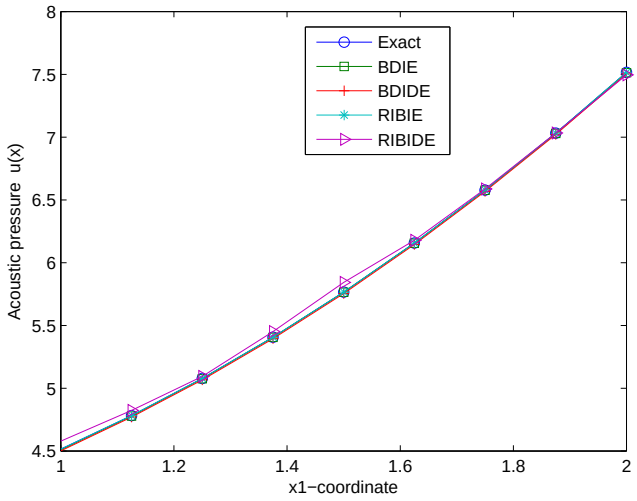

Fig. 20: Acoustic pressure distribution along the line $x_2 = 1.875$

9 Conclusion

In this paper, the BDIE/ BDIDE and RIBIE/RIBIDE formulations are derived and implemented for solving the two-dimensional Helmholtz equation with variable coefficients. Three different cases have been solved; when the parameter $a(x)$ is variable (with constant or variable wave number k), a parametrix is adopted in the formulation. However, when the parameter is constant (with variable wave number), the standard fundamental solution for the Laplace equation is used.

Numerical test examples show that accurate computational results can be achieved using both BDIE and BDIDE methods. The boundary and domain integrals in the formulations have a weak singularity. To calculate the boundary integrals we used a standard Gaussian quadrature rule. For the domain integrals, we have implemented a Gaussian quadrature rule with Duffy transformation by mapping the triangles into squares and eliminating the weak singularity. One of the most important advantages of the BEM is that no internal discretisation of the domain is required. This advantage, however, is generally lost for both BDIE and BDIDE methods.

Using the Radial Integration Method (RIM), it is possible to transform the domain integrals that appear in both BDIE and BDIDE methods into equivalent boundary integrals, thus retaining the boundary-only character of the standard BEM. Moreover, the RIM removes the weak singularities appearing in both domain integrals, simplifying and speeding up the calculation of the integrals. Numerical results showed that both the RIBIE and RIBIDE methods are able to generate accurate solutions in good agreement with BDIE and BDIDE results.

References

[1] Shouxin W., Xiping L., Tianguo P., Zhongshcng Z., Suh Z. The BEM for solving the nonhomogeneous Helmholtz equation with variable coefficients, Applied Mathematics and Mechanics 1996; 17:85-89.

[2] Rangogni R. The solution of the nonhomogeneous Helmholtz equation by means of the boundary element method, Appl. Math. Modelling 1984; 8:442-444.

[3] Ang WT. A beginner's course in boundary element methods. Boca Raton, USA: Universal Publishers; 2007.

[4] Paris F, Canas J. Boundary element method fundamentals and applications. New York: Oxford University Press: 1997.

[5] Brebbia CA., Telles JCF, Wrobel LC. Boundary element techniques. Berlin: Springer; 1984.

[6] Wrobel LC. The boundary element method, vol.1, Chichester: Wiley; 2002.

[7] Blyth M.G., Pozrikidis C. A comparative study of the boundary and finite element methods for the Helmholtz equation in two dimensions, Engineering Analysis with Boundary Elements 2007; 31:35-49.

[8] Clements DL. Fundamental solutions for second order linear elliptic partial differential equations. Computational Mechanics 1998; 22:26-31.

[9] Ang WT, Kusuma J, Clements DL. A boundary element method for a second order elliptic partial differential equation with variable coefficients. Engineering Analysis with Boundary Elements 1996; 18:311-316.

[10] Shaw RP. Green's functions for heterogeneous media potential problems. Engineering Analysis with Boundary Elements 1994; 13:219-221.

[11] Shaw RP, Gipson GS. A BIE formulation of a linearly layered potential problem. Engineering Analysis with Boundary Elements 1995; 16:1-3.

[12] Nardini D, Brebbia CA. A new approach for free vibration analysis using boundary elements. In Boundary Element Methods in Engineering, Brebbia CA (ed.). Springer: Berlin, 1982; 312-326.

[13] Partridge PW, Brebbia CA, Wrobel LC. The Dual Reciprocity Boundary Element Method. Computational Mechanics Publications: Southampton, 1992.

[14] Gao XW. The radial integration method for evaluation of domain integrals with boundary-only discretization. Engineering Analysis with Boundary Elements 2002; 26:905-916.

[15] Gao XW. A boundary element method without internal cells for two-dimensional and three-dimensional elastoplastic problems. Journal of Applied Mechanics (ASME) 2002; 69:154-160.

[16] Venturini WS. Further develpments of boundary element formulation for zoned domain problems. In C.A Brebbia, J.J. Connor(eds), Advances in Boundary Elements, Computational Mechanics Publications, Southampton and Springer-Verlag, Berlin and New York; 1989; pp.25l-267.

[17] Brunton I. Solving Variable Coefficient Partial Differential Equations Using the Boundary Element Method. PhD thesis, University of Auckland, New Zealand;1996.

[18] AL-Jawary MA, Wrobel LC, Maischak M. Numerical solution of a Dirichlet problem with variable coefficients by the boundary-domain integro-differential equation method. In: Lesnic D., editor. Eighth UK Conference on Boundary Integral Methods, University of Leeds Press; 2011. p. 25-32.

[19] AL-Jawary MA, Wrobel LC, Maischak M. Numerical solution of a Neumann problem with variable coefficients by the boundary-domain integral equation method. In: Lesnic D., editor. Eighth UK Conference on Boundary Integral Methods, University of Leeds Press; 2011. p. 33-40.

[20] AL-Jawary MA, Wrobel LC. Numerical solution of two-dimensional mixed problems with variable coefficients by the boundary-domain integral and integro-differential equation methods. Engineering Analysis with Boundary Elements 2011; 35:1279-1287.

[21] Mikhailov SE. Localized boundary-domain integral formulations for problems with variable coefficients. Engineering Analysis with Boundary Elements 2002; 26:681-690.

[22] Mikhailov SE, Nakhova IS. Mesh-based numerical implementation of the localized boundary-domain integral equation method to a variable-coefficient Neumann problem. Journal of Engineering Mathematics 2005; 51:251-259.

[23] Gao XW. A meshless BEM for isotropic heat conduction problems with heat generation and spatially varying conductivity. International Journal for Numerical Methods in Engineering 2006; 66:1411-1431.

[24] Fata SN. Treatment of domain integrals in boundary element methods. Applied Numerical Mathematics 2010, doi:10.1016/j.apnum.2010.07.003.

[25] Marin L., Elliott L., Heggs P.J., Ingham D.B., Lesnic D., Wen X. Dual reciprocity boundary element method solution of the Cauchy problem for Helmholtz-type equations with variable coefficients, Journal of Sound and Vibration 2006; 297:89-105.

[26] AL-Jawary MA,Wrobel LC. Radial integration boundary integral and integro-differential equation methods for two-dimensional heat conduction problems with variable coefficients, Engineering Analysis with Boundary Elements 2012; 36:685-695.

[27] Bridges T.R., Wrobel L.C. A dual reciprocity formulation for elasticity problems with body forces using augmented thin plate splines. Communications in Numerical Methods in Engineering 1996; 12:209-220.

[28] Karur SR., Ramachandran PA. Augmented thin plate spline approximation in DRM. Boundary Elements Communications 1995; 6:55-58.